Research article

Suppression of gastric cancer cell proliferation by miR-494-3p inhibitor-loaded engineered exosomes

Limin Zhang, Yingwei Xue, Hongfeng Zhang [*]

Department of Gastrointestinal Surgery, Harbin Medical University Cancer Hospital, No.150, Haping Road, Nangang District, Harbin, 150081, Heilongjiang Province, China

A B S T R A C T

Background: Gastric cancer necessitates novel treatments, and exosomes are promising therapeutic carriers. We created miR-494-3p inhibitor exosomes to assess their effects on gastric cancer cells.
Methods: We conducted a comprehensive investigation into the expression of the oncogenic miR-494-3p in gastric cancer tissues from patients. Subsequently, we engineered miR-494-3p inhibitor-loaded exosomes and characterized their morphology and size through transmission electron microscopy and nanoparticle tracking analysis. We next determined the encapsulation efficiency of the miR-494-3p inhibitor within these exosomes and evaluated the exosomes' structural integrity by quantifying the presence of exosomal markers. Following these validations, we co-cultured miR-494-3p inhibitor exosomes with cancer cells and employed PKH26 staining to visualize the efficient endocytosis of engineered exosomes by gastric cancer cells and assess the impact of these modified exosomes on gastric cancer cell proliferation, apoptosis, migration, and invasion.
Results: Increased expression of miR-494-3p was observed in gastric cancer tissues as compared to controls. Significant low miR-494-3p levels were found within miR-494-3p inhibitor exosomes, signifying effective encapsulation. The incorporation of miR-494-3p inhibitor into engineered exosomes did not alter exosome morphology or size. Finally, PKH26-stained exosomes clearly demonstrated efficient endocytosis by gastric cancer cells, leading to reduced proliferation, migration, invasion, and increased apoptosis.
Conclusion: Our study identifies elevated miR-494-3p in gastric cancer tissues prompting the development of miR-494-3p inhibitor-loaded exosomes with efficient encapsulation. These engineered exosomes demonstrate successful endocytosis by cancer cells. This highlights their potential for therapeutic use in gastric cancer treatment by suppressing proliferation, migration, and invasion while enhancing apoptosis.

1. Introduction

The incidence of gastric cancer (GC) has underwent a decline in recent decades, primarily attributed to improvements in socio-economic conditions and enhanced hygiene practices, leading to a decrease in Helicobacter pylori (HP) infection rates [1–3]. However, gastric cancer continues to hold its position as the fifth most common cancer worldwide and the fourth leading cause of cancer-related

mortality [4,5]. With a male-to-female incidence ratio of 2:1, it predominantly affects individuals over the age of 50. Despite these trends, early diagnosis rates for gastric cancer in China remain suboptimal. The prognosis of gastric cancer is influenced by various factors, including disease stage, location, tissue type, biological behavior, and treatment approaches [6]. China grapples with a substantial disease burden attributed to gastric cancer, standing as the second most commonly diagnosed cancer and the second leading cause of cancer-related mortality [7]. Significantly, regional variations in gastric cancer incidence manifest, with elevated rates in the northwest and eastern coastal regions in contrast to the southern regions of China [8–10]. Despite conventional therapies for advanced unresectable or recurrent gastric cancer, the median survival typically ranges from 12 to 15 months [11]. Therefore, developing new treatments for gastric cancer is crucial.

Exosomes, small circular membrane vesicles with diameters ranging from 30 nm to 150 nm, are generated by cells through various physiological or pathological processes, such as endocytosis and fusion [12–14]. Exosomes offer a promising avenue for enhancing cancer treatment efficacy by enabling precise drug delivery to tumor cells [15,16]. They can be loaded with both small molecules and macromolecules, making them valuable therapeutic tools for treating diseases, including cancers [17–20]. Given the substantial direct and indirect costs associated with certain types of cancers [21], there is a pressing need for advancements in medical approaches to cancer prognosis and therapy. The multifunctional nature of exosomes positions them as promising tools to address these challenges and propel progress in cancer treatment strategies. Exosomes exhibit favorable characteristics, including an extended circulating half-life, inherent tissue-targeting ability, biocompatibility, and minimal or no associated toxicity concerns [22]. Exosomes have emerged as valuable tools for diagnosing and treating inflammatory bone diseases [23]. Zhang's research has opened up new possibilities by revealing the potential of exosome-like structures in advancing treatment options for inflammatory bowel diseases [24]. Additionally, Wang et al. have delved into the role of exosomes in addressing neurodegenerative conditions, including Alzheimer's disease [25]. Exosomes containing miR-21-3p have shown promise in alleviating atherosclerosis [26] and Qu demonstrated that exosome-derived miR-181-5p can protect against liver fibrosis by promoting autophagy [27]. Additionally, engineered exosomes encapsulating miRNAs have shown efficacy in cancer treatment, efficiently delivering antitumor drugs to tumor sites without equivalent side effects of free drugs [28–31]. These engineered exosomes have high encapsulation efficiency and can slow tumor growth *in vivo* [32]. They have been used to block the malignant behavior of glioblastoma multiforme cells, induce apoptosis in ovarian cancer cells, and inhibit gastric cancer progression [33–39]. Additionally, few studies also focused on delivering of exosomes loaded with inhibitors of miRNA for disease treatment [40,41]. In summary, exosomes hold promise as potential drug carriers for cancer treatment.

The role of miRNA-494-3p in tumorigenesis has sparked controversy [42]. It has been identified as an onco-miRNA in diverse carcinomas, including lung cancer [43] and breast cancer [44], exerting effects on cancer cell proliferation and *in vivo* metastasis. Furthermore, miRNA-494-3p displays significant overexpression in non-small-cell lung cancer, endometrial cancer, and bladder cancer [45–47]. Additionally, it contributes to the enahnced growth, migration, and invasion of nasopharyngeal carcinoma through the targeting of Sox7 [42]. However, there has been no investigation into the effects of exosomes loaded with miR-494-3p inhibitors on gastric cancer cells. Therefore, our aim is to explore this uncharted territory, potentially providing a novel intervention strategy for future gastric cancer treatment.

2. Materials and methods

2.1. Clinical tissue collection

We collected 22 gastric cancer tissues from patients and 22 healthy tissues from individuals undergoing surgery at Harbin Medical University Cancer Hospital. None of the patients had received any tumor-specific therapy before their diagnoses, and pathologists verified all the diagnoses. The patients ranged from 18 to 70 years old. This research was approved by the ethics committee of the cancer hospital at Harbin Medical University (2019-164-R), and written informed consent was obtained from each participant. Prior to use, the tissues were stored at −80 °C.

2.2. Cell

The normal human gastric cell line GES-1 and five gastric cancer cell lines, HGC-27, NCI–N87, MKN-45, SNU-1 and MKN-7 were obtained from Procell (Wuhan, China) and cultured in F12K medium (Biological Industries, Israel) supplemented with 1 % penicillin/ streptomycin (Yeasen, China) and 10 % fetal bovine serum (Royacel, Lanzhou). Cells were maintained in a 5 % CO_2 atmosphere at 37 °C until they reached 80 % confluency.

2.3. Exosome extraction and characterization using transmission electron microscopy

Human bone marrow mesenchymal stem cells were processed for exosome extraction and purification using an exosome extraction kit (Umibio, China) following the manufacturer's instructions. The cells were treated for 16 h at 4 °C, and the remaining exosome-containing solution was then transferred to a purification column and centrifuged at $1500 \times g$ for 30 min to collect the exosomes. Subsequently, the exosomes in the collection column were eluted with the provided eluent. After extraction, the exosomes were initially rinsed twice with 100 μl of phosphate-buffered solution, fixed using 2 % paraformaldehyde followed by 2 % glutaraldehyde, and then placed on a 200-mesh Cu grid coated with carbon-Formvar film (ProSciTech, Kirwan, QLD, Australia). They were allowed to absorb for 5 min, and any excess solution was removed by blotting the edge of each grid with filter paper. Finally, the exosomes were

stained with 20 μl of 2 % uranyl acetate in water at room temperature for 2–3 min and photographed using transmission electron microscopy (TEM, Tecnai G2 Spirit Bio Twin, FEI) at 100 kV.

2.4. Nanoparticle tracking analysis (NTA)

NTA was employed to determine the size distribution and concentration of exosomes. Briefly, exosomes were resuspended in 1 mL of trehalose pulse medium (TPM). It is worth noting that trehalose pulse medium has recently been demonstrated to preserve the structural integrity of melanoma exosomes [48]. The concentration and size of the exosomes were detected utilizing nanoparticle tracking analysis (ZetaView PMX 110 Germany) according to the operation protocol reported previously [49].

2.5. Exosome visualization

Exosomes were labeled with the red fluorescent dye PKH26, which binds to lipid membranes, using a PKH26 staining buffer (Umibio, China). Briefly, 100 μg of exosomes was mixed with 50 μL of PKH26 dye and incubated in the dark. To stop the labeling reaction, 1 mL of PBS containing 1 % BSA was added, and the labeled exosomes were re-isolated using Exoquick precipitation solution. Subsequently, these labeled exosomes were co-cultured with cancer cells, and their _in vitro_ tracking was visualized using a confocal microscope (Carl Zeiss, Germany).

2.6. Loading of miR-494-3p inhibitor

The miR-494-3p inhibitor was procured from Ribobio (Guangzhou, China) and introduced into exosomes via electroporation. In brief, the electroporation process involved the mixing of 500 nmol of miR-494-3p inhibitor and 500 μl of electroporation buffer (BTX, USA). This mixture was then transferred to a 0.4 cm electrode cup for electroporation using a MicroPulser (Bio-RAD, USA) set at 200 V and 100 μF. Following electroporation, the mixture underwent centrifugation at 4 °C and 100,000 g for 70 min to eliminate any unloaded miR-494-3p inhibitor. The resulting exosomes loaded with miR-494-3p inhibitor were resuspended in PBS and preserved through cryopreservation.

2.7. qPCR assay

Cellular or exosomal total RNA was extracted utilizing ISOLATION TRIzol buffer® (Multi Sciences, Hangzhou), followed by cDNA synthesis from the reverse-transcribed RNA using the RT-PCR Kit (Yeasen, China) following the manufacturer's instructions. Quantitative real-time PCR (qRT-PCR) was performed using the PerfectStart® Sybr qPCR Mix (Vazyme, Nanjing). Expression levels were determined using the $2^{-\Delta\Delta Ct}$ method. The primers for miR-494-3p and U6 were as follows.

Gene	Forward seq	Reverse seq
U6	5′-AGGCTTGCTGCTCGGCAGTTGAT-3′	5′-AAGCTAGCTGATCGATCGCTCT-3′
mi-494-3p	5′-TGAAACATACACGGGAACCA-3′	5′-ATGCTGCTAGCTGATCGCTAGCT-3′

2.8. Cell apoptosis

Cell apoptosis was assessed using an Annexin V-7AAD apoptosis detection kit following the manufacturer's instructions. In brief, 2×10^5 HGC27 cells in each treatment group, including the PBS group, unloaded Exo, and exosomes loaded with the miR-494-3p inhibitor, were collected and rinsed twice with PBS. Each cell pellet was suspended in 350 μL of PBS at a concentration of 2 million cells (2×10^6 cells/mL), followed by the addition of 100 μL of incubation buffer containing 2 μL of annexin V and 2 μL of 7AAD to each experimental group. Subsequently, cell apoptotic rates were analyzed using flow cytometry (Canto II, BD) within 1 h.

2.9. EdU assay

The proliferation of HGC27 cells was assessed using the Edu kit (Thermo Fisher, USA). HGC27 cells were seeded in 96-well plates at a density of 4×10^4 cells/well and treated with PBS, unloaded exosomes, or miR-494-3p inhibitor-loaded exosomes for a minimum of 6 h. Following treatment, the cells were co-cultured with 10 μM EdU reagent (Thermo Fisher, USA) for 2.5 h. Subsequently, the HGC27 cells were fixed and permeabilized using 0.3 % Triton X-100 and then incubated with FITC solution for 1 h. The HGC27 cells were thoroughly rinsed with PBS three times. Finally, nuclear staining was performed using Hochest 33342 (Fcmacs, China), and cell counting was carried out using a fluorescence microscope (CKX53, Olympus).

2.10. Wound healing

HGC27 cells were subjected to treatment with PBS, unloaded exosomes, or miR-494-3p inhibitor-loaded exosomes for 24 h, and these cells were subsequently cultured in 24-well plates until reaching approximately 85 % confluence. Uniform wounds were created

horizontally using a 200 µl pipette tip to ensure consistent wound strength and width. After aspirating the supernatant, the cells were washed twice with PBS to eliminate floating cells. Following this, FBS-free medium was added, and the percentage of scratch healing was assessed after 48 h using IPP software.

2.11. Transwell assay

To evaluate cell migration and invasion, we conducted experiments utilizing a transwell chamber with 8 µm pores (Merck, USA). In the lower chamber of each well, 500 µL of culture medium containing 10 % FBS was introduced as a chemoattractant. HGC27 cells subjected to exosome treatment (specifically, 2×10^4 cells in a 300 µL suspension) were carefully placed into the upper chamber. This upper chamber had been prepared beforehand with a coating of matrix gel. Subsequently, the plates were incubated under standard conditions at 37 °C for a period of 24 h. The cells which migrated to the lower surface of the membrane were meticulously fixed with 4 % paraformaldehyde and subsequently stained using a solution containing crystal violet (Alladin, China). Microscopic images were thoughtfully captured in a random fashion across ten distinct fields (10 × magnification). Furthermore, for cell invasion assays, we executed a procedure akin to the migration assay, and the difference is that transwell chambers had been coated with Matrigel. The final results were determined after a 24-h period, capturing the count of cells that effectively traversed the Matrigel matrix.

2.12. Western blot

Proteins were extracted from HGC27 cells using a protein extraction kit (Tiangen Biotech, Beijing, China). The protein concentrations were determined using the Bradford method. Subsequently, protein samples (35 µg) were separated through 10 % sodium dodecyl sulfate-polyacrylamide gel electrophoresis (SDS-PAGE) and transferred onto a nitrocellulose membrane (Whatman, USA). The membranes were then incubated overnight at 4 °C with primary antibodies (Arigo, Taiwan, China) against Bax (ARG#66247), Bcl-2 (ARG#55188), Cleaved-caspase3 (ARG#57512), Cleaved-caspase9 (CST#9505), MMP2 (ARG#56426), and MMP9 (ARG#54980). β-actin (Actb, ARG#62346) served as the control protein. Following overnight incubation, the membranes were blocked with 5 % non-fat milk powder (BD, USA) and probed with anti-rabbit horseradish peroxidase-labeled IgG secondary antibody (ARG65351, Arigo, Taiwan, China) and anti-mouse secondary antibody for MMP9 (CST #7076). Immunoreactive bands were visualized using the Clarity Western ECL kit (Bio-Rad).

2.13. Statistical analysis

The data obtained from three independent repetitions are presented as the mean ± standard deviation (SD). Statistical analysis involved the use of Student's t-test to assess the difference between two cohorts. For comparisons involving three or more groups, one-way analysis of variance (ANOVA) was employed. The statistical difference is indicated by $P < 0.05$.

3. Results

3.1. The expression of miR-494-3p in normal and gastric cancer cells

The level of miR-494-3p was assessed in gastric cancer tissues and cell lines through qPCR analysis. The results revealed a higher abundance of miR-494-3p in the cancerous tissue of gastric cancer pateints compared to the control group (Fig. 1A). Furthermore, miR-494-3p exhibited significant expression across five gastric cancer cell lines when compared to GES-1 cells, with HGC27 cells displaying the highest miR-494-3p levels than other cancer cells (Fig. 1B). Collectively, these findings indicate an upregulation of miR-494-3p in gastric cancer.
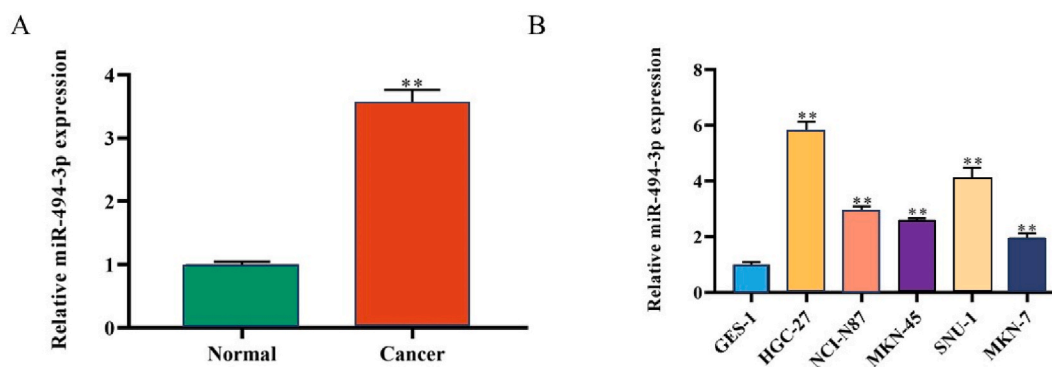
Fig. 1. The expression level of miR-494-3p in gastric cancer. (A) The level of miR-494-3p in cancer tissues. (B) qPCR was used to assess the level of miR-494-3p in cancer cells. Data are shown as average ± SD of triple standalone experiments. **p < 0.01 compared with normal or GES-1 group.

3.2. Identification of engineered exosome

We extracted, and purified miR-494-3p inhibitor-loaded exosomes, followed by engineering these exosomes. Examination of their morphology through TEM revealed no discernible differences between engineered miR-494-3p inhibitor-loaded exosomes and unloaded exosomes (Fig. 2A). Furthermore, particle size analysis using NTA demonstrated a consistent size of approximately 100 nm for both engineered and unloaded exosomes (Fig. 2B). These results from TEM and NTA collectively suggested that the incorporation of miR-494-3p did not alter the morphology or size of exosomes. To ensure the integrity of exosomes, we assessed the presence of exosomal markers, TSG101 and CD63, via Western blot analysis in both unloaded and miR-494-3p inhibitor exosomes. Importantly, these markers were absent in HGC-27 cells (Fig. 2C). Additionally, we evaluated the loading efficiency of the miR-494-3p inhibitor within exosomes using qRT-PCR. The data showed that miR-494-3p expression was significantly lower in miR-494-3p inhibitor exosomes compared to unloaded exosomes, indicating effective encapsulation (Fig. 2D).

3.3. Engineered exosome was endocytosed by gastric cancer cells

Following the development of engineered exosomes, it is imperative to assess their uptake by gastric cancer cell lines. To facilitate this evaluation, we labeled the exosomes with PKH26 and subsequently co-cultured them with HGC27 cells. Using confocal microscopy, we visualized PKH26-labeled exosomes, as depicted in Fig. 3A. This confirmed the specific uptake of both unloaded exosomes and miR-494-3p inhibitor-loaded exosomes by HGC27 gastric cancer cells (Fig. 3A). Furthermore, we observed a notable reduction in the levels of miR-494-3p within HGC27 cells following the uptake of miR-494-3p engineered exosomes, in comparison to the unloaded exosomes (Fig. 3B). This observation strongly indicates the successful endocytosis of engineered exosomes by gastric cancer cells.

3.4. Engineered exosomes enhanced the apoptosis and inhibited the proliferation of gastric cancer cells

We investigated the impact of engineered exosomes on the proliferation and apoptosis of gastric cancer cells. In the miR-494-3p inhibitor exosome group, there were fewer EdU-positive cells compared to the PBS group and the unloaded exosome group (Fig. 4A). Flow cytometry analysis demonstrated that miR-494-3p inhibitor exosomes significantly increased the apoptotic ratio of
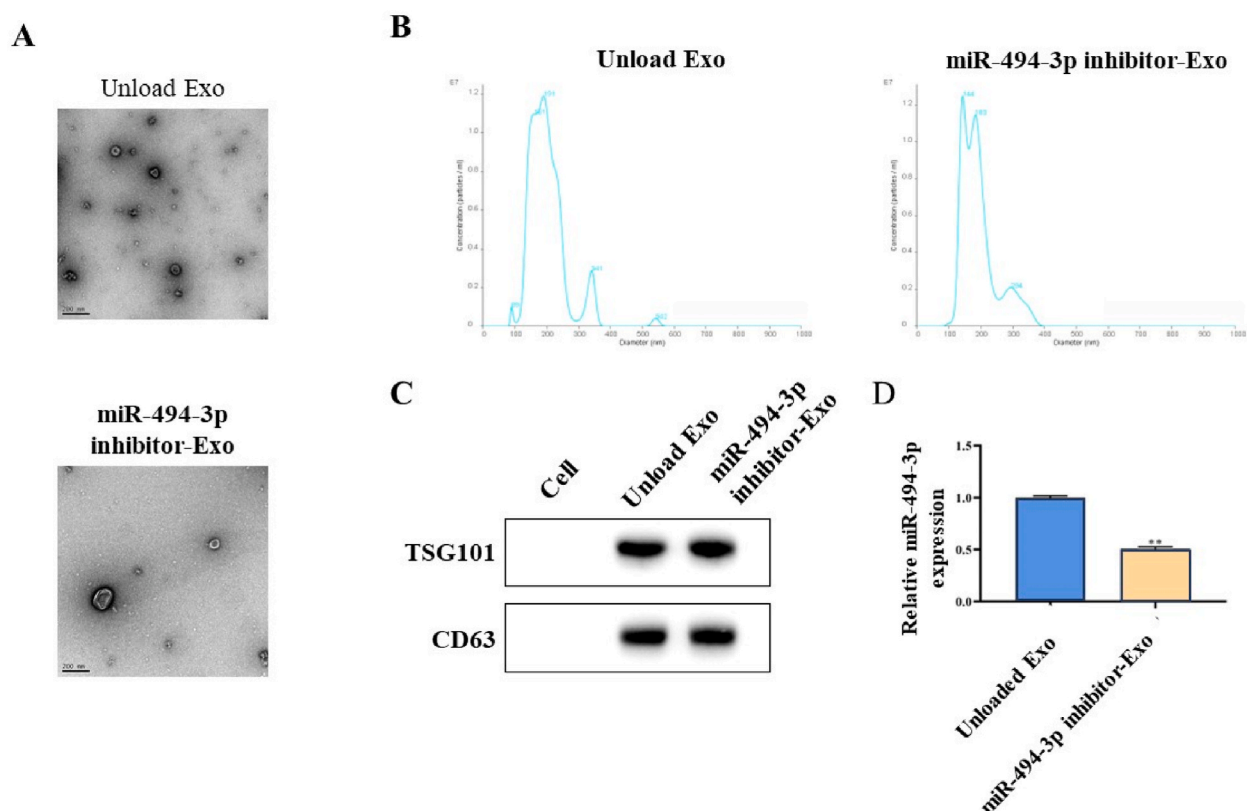
Fig. 2. Extraction and identification of engineered exosome. (A) TEM was conducted to determine the morphology of the exosome. (B) The particle size of the exosome was detected by NTA. (C) The protein level of exosome marker was shown. Full blots were shown in supplementray file S1. (D) qPCR was used to detect the expression of miR-494-3p in unloaded and engineered exosomes. Data are shown as average ± SD of triple standalone experiments. **p < 0.01 compared with unloaded exosome group.
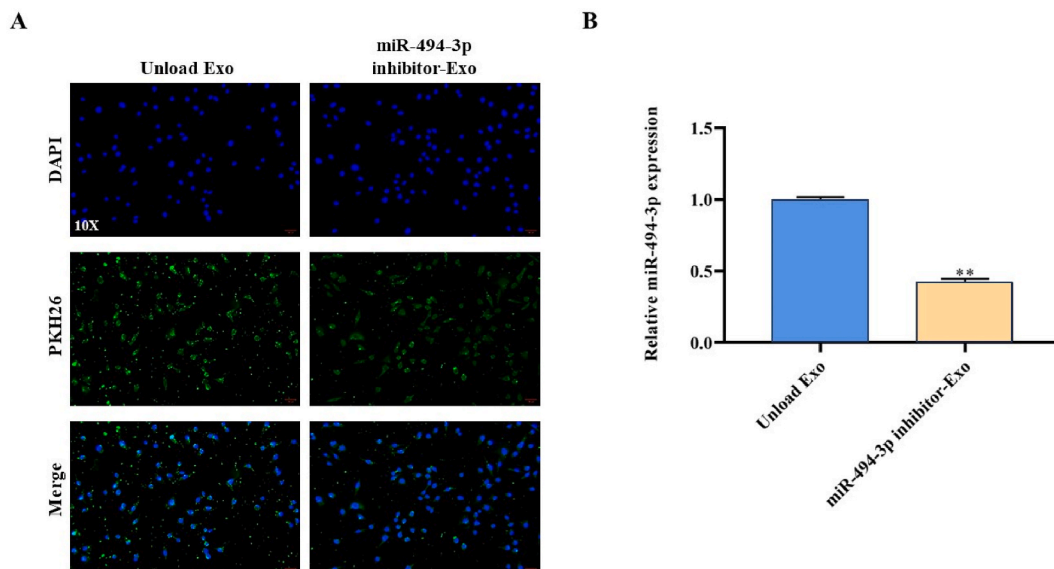
Fig. 3. Assessment of Engineered Exosome Uptake by Cells. *(A) Micrograph showing PKH26-labeled exosomes. (B) qPCR analysis of miR-494-3p expression in HGC27 cells following exosome uptake. Data represents the mean ± SD from three independent experiments. **p < 0.01 compared with unloaded exosome group.*
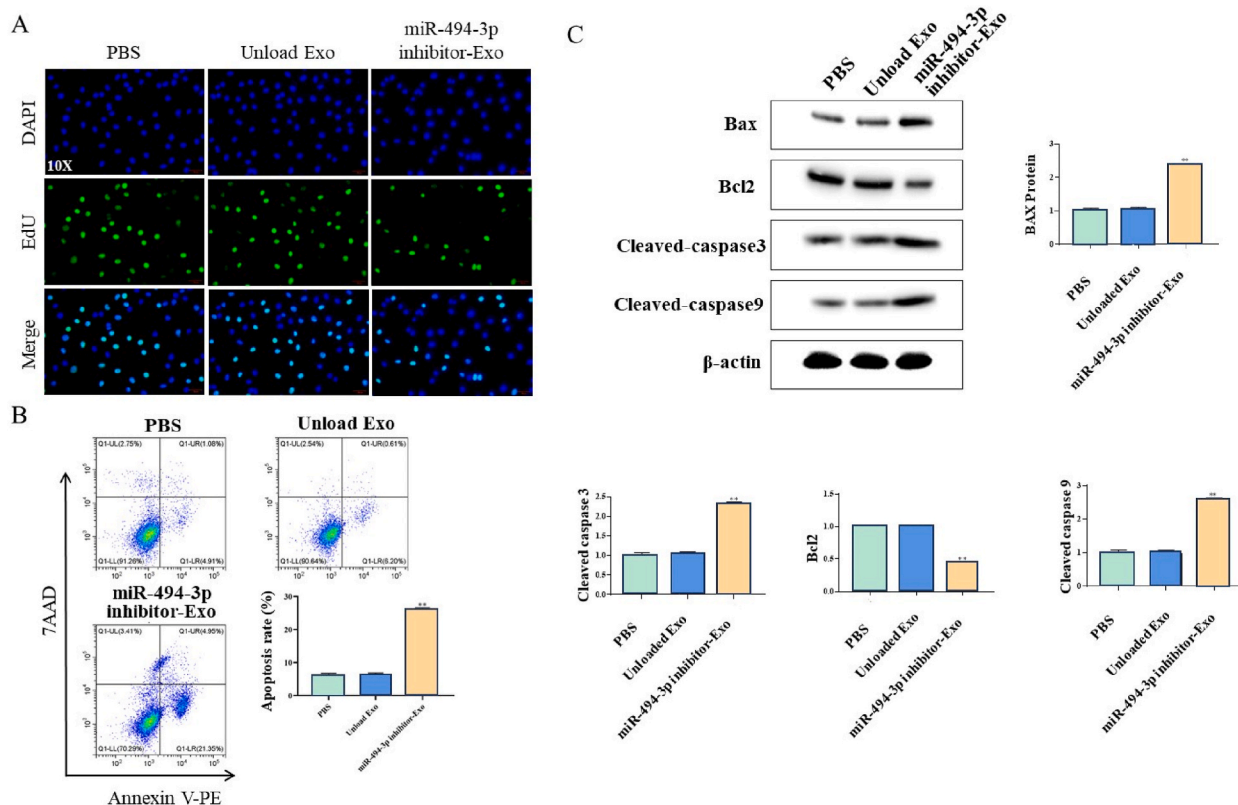
Fig. 4. Effect of engineered exosome on proliferation and apoptosis of cancer cells. (A) The proliferation was detected by EdU assay. (B) Flow cytometry was used to assess cell apoptosis. (C) The level of apoptotic and antiapoptotic protein was detected by Western blot assay. Full blots were shown in supplementray file S1. Data are shown as average ± SD of triple standalone experiments. **p < 0.01 compared with unloaded exosome group.

HGC27 cells (Fig. 4B). Western blot analysis of apoptosis-related protein levels revealed higher levels of Bax, cleaved-caspase 3, and cleaved-caspase 9 in the engineered exosome group, while the levels of the antiapoptotic protein Bcl2 were lower (Fig. 4C). In summary, engineered exosomes suppressed the proliferation and enhanced the apoptosis of gastric cancer cells.

3.5. Engineered exosomes suppressed the motility of gastric cancer cells

To assess the influence of engineered exosomes on the motility of gastric cancer cells, wound healing and transwell assays were conducted. The miR-494-3p inhibitor exosomes impeded the wound healing process of HGC27 cells when compared to the PBS and unengineered exosome groups (Fig. 5A). Results from transwell assays revealed that HGC27 cells treated with miR-494-3p inhibitor-loaded exosomes exhibited decreased migration and invasion in comparison to cells treated with unloaded exosomes and PBS (Fig. 5B). To further elucidate the reduction in metastatic potential conferred by miR-494-3p inhibitor exosomes, we examined the levels of metastasis-related proteins. Western blot results demonstrated diminished levels of SOX7, MMP2, and MMP9 in the engineered exosome group in comparison to the unloaded exosome and PBS control groups (Fig. 5C). Additionally, we prepared miR-494-3p mimic-loaded exosomes and treated HGC27 cells, revealing that, in comparison with unloaded exosomes, miR-494-3p mimic-loaded exosomes increased proliferation, migration, invasion, and suppressed apoptosis in HGC27 cells (Supplementary Fig. 1).

4. Discussion

Numerous drug nanoparticles have been created in an effort to enhance the therapeutic efficacy of medications. Unfortunately,
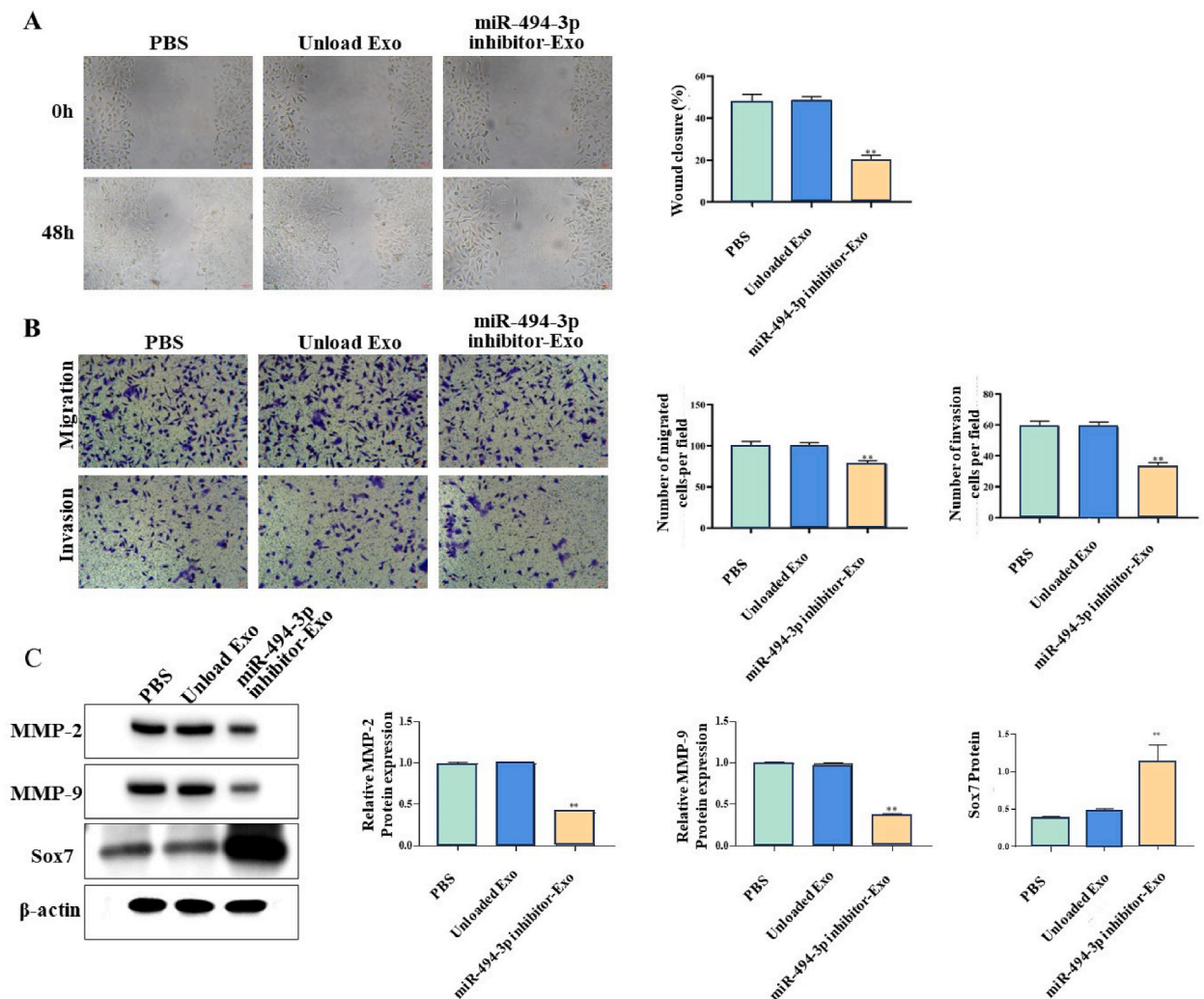
Fig. 5. Effect of miR-494-3p inhibitor-loaded exosome on motility of cancer cells. (A) The wound healing assay of cancer cells. (B) The migration and invasion ability of cells was detected by transwell. (C) The level of SOX7, MMP2 and MMP9 was detected by Western blot. Full blots were shown in supplementrary file S1. Data are shown as average ± SD of triple standalone experiments. **$p < 0.01$ compared with unloaded exosome group.

toxicity and efficient clearance by the mononuclear phagocyte system are two distinct issues with drug nanoparticles caused by the opsonization of drug-loaded synthetic nanoparticles in the blood [50]. Exosomes are effective medication transporters because of their distinctive characteristics. Exosomes can deliver their cargo to target cells by adhering to them using a variety of surface adhesion proteins and carrier ligands [30,51]. In our research, we employed an approach to the therapy of cancer offered by exosomes as a carrier to conduct anti-tumor studies and found that exosomes could stop the growth of tumor cells when miRNA was encapsulated in them.

miRNA had been reported to play an important role in many anti-tumor studies [52,53]. More and more studies had reported that miRNAs can be released from exosomes, and exosomal miRNAs can be used in anti-tumor treatment [54–57]. Previous research has unveiled the multifaceted role of miR-494-3p in diverse cancer types. For instance, He et al. has reported that miR-494-3p functions as an oncogene, promoting growth, migration, and invasion of nasopharyngeal cancer cells [42]. In hepatocellular carcinoma, elevated miR-494-3p levels are associated with aggressive clinicopathological features and indicative of an unfavorable prognosis for patients [58]. Conversely, conflicting findings have emerged, suggesting a potential tumor-suppressive role for miR-494-3p. Studies have indicated that miR-494-3p may mitigate liver fibrosis, impede hepatic stellate cell proliferation, and induce apoptosis by targeting TRAF3 [59]. Similarly, it exhibits inhibitory effects in prostate cancer by targeting CXCR4, thereby suppressing proliferation, invasion, and migration of prostate cancer cells [60]. In our research, we scrutinized the augmented expression of miR-494-3p within gastric cancer cells. Subsequently, we embarked on encapsulating the miR-494-3p inhibitor within exosomes to assess its resilience and its impact on the proliferation, apoptosis, migration, and invasion of gastric cancer cells [30].

In the context of miRNA loading methods, various strategies have been employed in previous studies. For instance, Xue et al. utilized a genetic engineering approach to enhance miR-317b-5p expression within exosomes [38]. Huang et al., on the other hand, infected HEK293 cells with a miR-31-5p lentivirus vector to generate miR-31-5p-engineered exosomes [61]. Although transfection offers a straightforward means to obtain engineered exosomes, it may not guarantee optimal loading efficiency. In contrast, Kobayashi et al. used a quick and convenient electroporation method to load miRNA into exosomes, effectively inhibiting the progression of ovarian cancer [62].

In our study, we opted for the direct electroporation approach to load the miR-494-3p inhibitor into exosomes, resulting in a notably high loading efficiency. Subsequently, these exosomes were efficiently internalized by gastric cancer cells, leading to a substantial decrease in the levels of miR-494-3p within these cancerous cells. Following treatment with miR-494-3p inhibitor-loaded exosomes, we observed a remarkable suppression of proliferation, migration, and invasion in gastric cancer cells, alongside an exacerbation of apoptosis. These findings underscore the potential utility of exosomes encapsulated with the miR-494-3p inhibitor for the treatment of gastric cancer cells. Previous study demonstrated that miR-494-3p targets Sox7 and promotes proliferation, migration, and invasion ability in nasopharyngeal carcinoma [42]. Our study corroborated the inhibitory effect of miR-494-3p on Sox7 expression. Importantly, our findings suggest that the miR-494-3p inhibitor exosome regulates MMP2 and MMP9 by targeting Sox7, resulting in the transcriptional inactivation of MMP2 and MMP9, consistent with previous research.

While these findings hold significant promise, it is crucial to acknowledge the study's limitations, particularly the absence of *in vivo* validation through animal models. Future research should explore the application of these exosomes in comprehensive animal models and xenograft experiments to further substantiate their therapeutic potential in the treatment of gastric cancer, encompassing both xenograft and metastasis models in mice.

5. Conclusion

In conclusion, our investigation sheds light on the elevated expression of miRNA-494-3p in gastric cancer tissues and cells, surpassing levels observed in normal controls. Employing miR-494-3p inhibitor-loaded exosomes, we achieved a substantial decrease in miRNA-494-3p within gastric cancer cells, resulting in a noteworthy suppression of proliferation, migration, and invasion, coupled with an enhancement of apoptosis. The study underscores the potential efficacy of exosomes encapsulating the miR-494-3p inhibitor as a promising therapeutic avenue for gastric cancer. This avenue of research presents a compelling opportunity for the prevention and treatment of gastric cancer, with exosomes emerging as a noteworthy carrier for targeted miR-494-3p therapy.

Data availability statement

The data that support the findings of this study are available from the corresponding author upon reasonable request.

Funding

Ethics approval and consent to participate

The experimental protocol was established according to the ethical guidelines of the *Helsinki Declaration* and was approved by the Ethics Committee of the Harbin Medical University Cancer Hospital (2019-164-R).

CRediT authorship contribution statement

Limin Zhang: Writing – review & editing, Visualization, Validation, Resources, Investigation, Data curation. **Yingwei Xue:** Writing – review & editing, Writing – original draft, Visualization, Validation, Project administration, Conceptualization. **Hongfeng Zhang:** Supervision, Resources, Methodology, Formal analysis, Conceptualization.

Declaration of competing interest

The authors declare that they have no known competing financial interests or personal relationships that could have appeared to influence the work reported in this paper.

Appendix A. Supplementary data

Supplementary data to this article can be found online at https://doi.org/10.1016/j.heliyon.2024.e30803.

References

[1] G. Luo, et al., Global patterns and trends in stomach cancer incidence: age, period and birth cohort analysis, Int. J. Cancer 141 (7) (2017) 1333–1344.
[2] O. Mashta, Stomach cancer incidence has halved over past 30 years in Britain, BMJ 339 (2009) b3281.
[3] Y. Qin, et al., Global burden and trends in incidence, mortality, and disability of stomach cancer from 1990 to 2017, Clin. Transl. Gastroenterol. 12 (10) (2021) e00406.
[4] H. Sung, et al., Global cancer statistics 2020: GLOBOCAN estimates of incidence and mortality worldwide for 36 cancers in 185 countries, CA A Cancer J. Clin. 71 (3) (2021) 209–249.
[5] J. Ferlay, et al., Cancer statistics for the year 2020: an overview, Int. J. Cancer (2021).
[6] F. He, Y. Sha, B. Wang, Relationship between alcohol consumption and the risks of liver cancer, esophageal cancer, and gastric cancer in China: meta-analysis based on case-control studies, Medicine (Baltim.) 100 (33) (2021) e26982.
[7] F.H. Wang, et al., The Chinese Society of Clinical Oncology (CSCO): clinical guidelines for the diagnosis and treatment of gastric cancer, 2021, Cancer Commun. 41 (8) (2021) 747–795.
[8] L. Yang, et al., The relative and attributable risks of cardia and non-cardia gastric cancer associated with Helicobacter pylori infection in China: a case-cohort study, Lancet Public Health 6 (12) (2021) e888–e896.
[9] Y. Zhang, J. Yu, The role of MRI in the diagnosis and treatment of gastric cancer, Diagn Interv Radiol 26 (3) (2020) 176–182.
[10] L. Zong, et al., The challenge of screening for early gastric cancer in China, Lancet 388 (10060) (2016) 2606.
[11] Y. Yoshinami, H. Shoji, Recent advances in immunotherapy and molecular targeted therapy for gastric cancer, Future Sci OA 9 (2) (2023) Fso842.
[12] L.M. Doyle, M.Z. Wang, Overview of extracellular vesicles, their origin, composition, purpose, and methods for exosome isolation and analysis, Cells 8 (7) (2019).
[13] C. He, et al., Exosome theranostics: biology and translational medicine, Theranostics 8 (1) (2018) 237–255.
[14] A. Almohammai, et al., Asthmatic condition induced the activity of exosome secretory pathway in rat pulmonary tissues, J. Inflamm. 18 (1) (2021) 14.
[15] M. Ahmadi, R. Abbasi, J. Rezaie, Tumor immune escape: extracellular vesicles roles and therapeutics application, Cell Commun. Signal. 22 (1) (2024) 9.
[16] J. Rezaie, T. Etemadi, M. Feghhi, The distinct roles of exosomes in innate immune responses and therapeutic applications in cancer, Eur. J. Pharmacol. 933 (2022) 175292.
[17] S.A. Shaban, J. Rezaie, V. Nejati, Exosomes derived from senescent endothelial cells contain distinct pro-angiogenic miRNAs and proteins, Cardiovasc. Toxicol. 22 (6) (2022) 592–601.
[18] R. Kalluri, V.S. LeBleu, The biology, function, and biomedical applications of exosomes, Science 367 (6478) (2020).
[19] F. Nazari-Khanamiri, et al., Tumor cells-derived exosomal noncoding RNAs in cancer angiogenesis: molecular mechanisms and prospective, Cell Biochem. Funct. 41 (8) (2023) 1008–1015.
[20] J. Rezaie, et al., Mesenchymal stem cells derived extracellular vesicles: a promising nanomedicine for drug delivery system, Biochem. Pharmacol. 203 (2022) 115167.
[21] S. Rezaei, M. Babaei, A systematic literature review on direct and indirect costs of triple-negative breast cancer, Cost Eff. Resour. Allocation 21 (1) (2023) 92.
[22] F. Aqil, R.C. Gupta, Exosomes in cancer therapy, Cancers 14 (3) (2022).
[23] Y. Hu, et al., Exosome: function and application in inflammatory bone diseases, Oxid. Med. Cell. Longev. 2021 (2021) 6324912.
[24] H. Zhang, et al., Exosome-Induced regulation in inflammatory bowel disease, Front. Immunol. 10 (2019) 1464.
[25] X. Wang, et al., The role of exosomal microRNAs and oxidative stress in neurodegenerative diseases, Oxid. Med. Cell. Longev. 2020 (2020) 3232869.
[26] J. Zhu, et al., Exosomes from nicotine-stimulated macrophages accelerate atherosclerosis through miR-21-3p/PTEN-mediated VSMC migration and proliferation, Theranostics 9 (23) (2019) 6901–6919.
[27] Y. Qu, et al., Exosomes derived from miR-181-5p-modified adipose-derived mesenchymal stem cells prevent liver fibrosis via autophagy activation, J. Cell Mol. Med. 21 (10) (2017) 2491–2502.
[28] Z. Naseri, et al., Exosome-mediated delivery of functionally active miRNA-142-3p inhibitor reduces tumorigenicity of breast cancer in vitro and in vivo, Int. J. Nanomed. 13 (2018) 7727–7747.
[29] S. Zhao, et al., Tumor-derived exosomal miR-934 induces macrophage M2 polarization to promote liver metastasis of colorectal cancer, J. Hematol. Oncol. 13 (1) (2020) 156.
[30] E.V. Batrakova, M.S. Kim, Using exosomes, naturally-equipped nanocarriers, for drug delivery, J. Contr. Release 219 (2015) 396–405.
[31] M. Zhang, et al., Engineered exosomes from different sources for cancer-targeted therapy, Signal Transduct. Targeted Ther. 8 (1) (2023) 124.
[32] M.D.A. Paskeh, et al., Emerging role of exosomes in cancer progression and tumor microenvironment remodeling, J. Hematol. Oncol. 15 (1) (2022) 83.
[33] H. Monfared, et al., Potential therapeutic effects of exosomes packed with a miR-21-sponge construct in a rat model of glioblastoma, Front. Oncol. 9 (2019) 782.
[34] H. Liu, et al., The effect of triptolide-loaded exosomes on the proliferation and apoptosis of human ovarian cancer SKOV3 cells, BioMed Res. Int. 2019 (2019) 2595801.
[35] X. Jing, et al., Exosome-transmitted miR-769-5p confers cisplatin resistance and progression in gastric cancer by targeting CASP9 and promoting the ubiquitination degradation of p53, Clin. Transl. Med. 12 (5) (2022) e780.
[36] S. Lin, et al., Exosome miR-3184-5p inhibits gastric cancer growth by targeting XBP1 to regulate the AKT, STAT3, and IRE1 signalling pathways, Asia Pac. J. Clin. Oncol. (2022).

[37] G. Liang, et al., Engineered exosome-mediated delivery of functionally active miR-26a and its enhanced suppression effect in HepG2 cells, Int. J. Nanomed. 13 (2018) 585–599.

[38] Q. Xue, et al., miR-371b-5p-Engineered exosomes enhances tumor inhibitory effect, Front. Cell Dev. Biol. 9 (2021) 750171.

[39] W. Zhou, et al., Engineered exosomes loaded with miR-449a selectively inhibit the growth of homologous non-small cell lung cancer, Cancer Cell Int. 21 (1) (2021) 485.

[40] J.J. Wang, et al., Macrophage-secreted exosomes delivering miRNA-21 inhibitor can regulate BGC-823 cell proliferation, Asian Pac. J. Cancer Prev. APJCP 16 (10) (2015) 4203–4209.

[41] C.J. Guo, et al., Exosome-mediated inhibition of microRNA-449a promotes the amplification of mouse retinal progenitor cells and enhances their transplantation in retinal degeneration mouse models, Mol. Ther. Nucleic Acids 31 (2023) 763–778.

[42] H. He, et al., MicroRNA-494-3p promotes cell growth, migration, and invasion of nasopharyngeal carcinoma by targeting Sox7, Technol. Cancer Res. Treat. 17 (2018) 1533033818809993.

[43] A. Faversani, et al., miR-494-3p is a novel tumor driver of lung carcinogenesis, Oncotarget 8 (5) (2017) 7231–7247.

[44] T. Macedo, et al., Overexpression of mir-183 and mir-494 promotes proliferation and migration in human breast cancer cell lines, Oncol. Lett. 14 (1) (2017) 1054–1060.

[45] D. Kazmierczak, et al., Elevated expression of miR-494-3p is associated with resistance to osimertinib in EGFR T790M-positive non-small cell lung cancer, Transl. Lung Cancer Res. 11 (5) (2022) 722–734.

[46] L. Zhu, et al., miR-494-3p promotes the progression of endometrial cancer by regulating the PTEN/PI3K/AKT pathway, Mol. Med. Rep. 19 (1) (2019) 581–588.

[47] X.H. Xu, et al., MicroRNA-494-3p facilitates the progression of bladder cancer by mediating the KLF9/RGS2 axis, Kaohsiung J. Med. Sci. 38 (11) (2022) 1070–1079.

[48] J.L. Hood, M.J. Scott, S.A. Wickline, Maximizing exosome colloidal stability following electroporation, Anal. Biochem. 448 (2014) 41–49.

[49] K.B. Johnsen, et al., Evaluation of electroporation-induced adverse effects on adipose-derived stem cell exosomes, Cytotechnology 68 (5) (2016) 2125–2138.

[50] A.M. Allahverdiyev, et al., Current aspects in treatment of breast cancer based of nanodrug delivery systems and future prospects, Artif. Cells, Nanomed. Biotechnol. 46 (sup3) (2018) S755–S762.

[51] Y. Zhang, et al., Exosome: a review of its classification, isolation techniques, storage, diagnostic and targeted therapy applications, Int. J. Nanomed. 15 (2020) 6917–6934.

[52] B. He, et al., miRNA-based biomarkers, therapies, and resistance in Cancer, Int. J. Biol. Sci. 16 (14) (2020) 2628–2647.

[53] T.X. Lu, M.E. Rothenberg, MicroRNA, J. Allergy Clin. Immunol. 141 (4) (2018) 1202–1207.

[54] Z. Sun, et al., Effect of exosomal miRNA on cancer biology and clinical applications, Mol. Cancer 17 (1) (2018) 147.

[55] X. Luo, et al., Exosomes-mediated tumor metastasis through reshaping tumor microenvironment and distant niche, J. Contr. Release 353 (2023) 327–336.

[56] H.M. Nail, et al., Exosomal miRNA-mediated intercellular communications and immunomodulatory effects in tumor microenvironments, J. Biomed. Sci. 30 (1) (2023) 69.

[57] L.A. Bravo-Vázquez, et al., Applications of nanotechnologies for miRNA-based cancer therapeutics: current advances and future perspectives, Front. Bioeng. Biotechnol. 11 (2023) 1208547.

[58] H. Lin, et al., MiR-494-3p promotes PI3K/AKT pathway hyperactivation and human hepatocellular carcinoma progression by targeting PTEN, Sci. Rep. 8 (1) (2018) 10461.

[59] H. Li, et al., MicroRNA-494-3p prevents liver fibrosis and attenuates hepatic stellate cell activation by inhibiting proliferation and inducing apoptosis through targeting TRAF3, Ann. Hepatol. 23 (2021) 100305.

[60] P.F. Shen, et al., MicroRNA-494-3p targets CXCR4 to suppress the proliferation, invasion, and migration of prostate cancer, Prostate 74 (7) (2014) 756–767.

[61] J. Huang, et al., Development of a novel RNAi therapy: engineered miR-31 exosomes promoted the healing of diabetic wounds, Bioact. Mater. 6 (9) (2021) 2841–2853.

[62] M. Kobayashi, et al., Exploring the potential of engineered exosomes as delivery systems for tumor-suppressor microRNA replacement therapy in ovarian cancer, Biochem. Biophys. Res. Commun. 527 (1) (2020) 153–161.